

# UC Santa Cruz

## UC Santa Cruz Previously Published Works

**Title**

The DEIMOS spectrograph for the Keck II Telescope: integration and testing

**Permalink**

<https://escholarship.org/uc/item/84m7z4h6>

**Journal**

Proceedings of SPIE, 4841(3)

**ISSN**

0277-786X

**Authors**

Faber, Sandra M  
Phillips, Andrew C  
Kibrick, Robert I  
[et al.](#)

**Publication Date**

2003-03-07

**DOI**

10.1117/12.460346

Peer reviewed

# PROCEEDINGS OF SPIE

[SPIDigitalLibrary.org/conference-proceedings-of-spie](https://spiedigitallibrary.org/conference-proceedings-of-spie)

## The DEIMOS spectrograph for the Keck 2 Telescope: Integration and testing

Sandra M. Faber, Andrew C. Phillips, Robert I. Kibrick, Barry Alcott, Steven L. Allen, et al.

Sandra M. Faber, Andrew C. Phillips, Robert I. Kibrick, Barry Alcott, Steven L. Allen, Jim Burrous, T. Cantrall, De Clarke, Alison L. Coil, David J. Cowley, Marc Davis, William T. S. Deich, Ken Dietsch, David Kirk Gilmore, Carol Ann Harper, David F. Hilyard, Jeffrey P. Lewis, Molly McVeigh, Jeffrey Newman, Jack Osborne, Ricardo Schiavon, Richard J. Stover, Dean Tucker, Vernon Wallace, Mingzhi Wei, Gregory Wirth, Christopher A.F. Wright, "The DEIMOS spectrograph for the Keck 2 Telescope: Integration and testing," Proc. SPIE 4841, Instrument Design and Performance for Optical/Infrared Ground-based Telescopes, (7 March 2003); doi: 10.1117/12.460346

**SPIE.**

Event: Astronomical Telescopes and Instrumentation, 2002, Waikoloa, Hawai'i, United States

# The DEIMOS spectrograph for the Keck II telescope: integration and testing

S. M. Faber<sup>a</sup>, A. C. Phillips<sup>a</sup>, R. I. Kibrick<sup>a</sup>, B. Alcott<sup>a</sup>, S. L. Allen<sup>a</sup>, J. Burrous<sup>a</sup>,  
T. Cantrall<sup>a</sup>, D. A. Clarke<sup>a</sup>, A. L. Coil<sup>b</sup>, D. J. Cowley<sup>a</sup>, M. Davis<sup>b</sup>, W. T. S. Deich<sup>a</sup>,  
K. Dietsch<sup>a</sup>, D. K. Gilmore<sup>a</sup>, C. A. Harper<sup>a</sup>, D. F. Hilyard<sup>a</sup>, J. P. Lewis<sup>a</sup>, M. M. McVeigh<sup>a</sup>,  
J. Newman<sup>b</sup>, J. Osborne<sup>a</sup>, R. P. Schiavon<sup>a</sup>, R. J. Stover<sup>a</sup>, D. Tucker<sup>a</sup>, V. Wallace<sup>a</sup>,  
M. Z. Wei<sup>a</sup>, G. D. Wirth<sup>c</sup>, and C. A. Wright<sup>a</sup>

<sup>a</sup>UCO/Lick Observatory, University of California, Santa Cruz, CA 95064

<sup>b</sup>Department of Astronomy, University of California, Berkeley, CA 94720

<sup>c</sup>W. M. Keck Observatory, Kamuela, HI 96743

## ABSTRACT

The DEIMOS spectrograph is a multi-object spectrograph being built for Keck II. DEIMOS was delivered in February 2002, became operational in May, and is now about three-quarters of the way through its commissioning period. This paper describes the major problems encountered in completing the spectrograph, with particular emphasis on optical quality and image motion. The strategies developed to deal with these problems are described. Overall, commissioning is going well, and it appears that DEIMOS will meet all of its major performance goals.

**Keywords:** Astronomical spectrographs, multi-object spectrographs, astronomical cameras, ground-based instrumentation, CCDs, mosaic detectors, flexure compensation, optical testing

## 1. INTRODUCTION

DEIMOS (which stands for DEep Imaging Multi-Object Spectrograph) is a multi-object spectrograph recently built for the Keck II telescope<sup>1–3</sup>. DEIMOS represents an advance in the state of the art of MOS spectrographs in several ways. Its optical components are large—the slitmasks are 28 inches long and span 16.6' on the sky; the camera has lenses up to 13 inches in diameter, three steep aspherics, three CaF<sub>2</sub> elements, and weighs 600 lb. The detector consists of a mosaic of 8 2K×4K custom-designed red-sensitive CCDs from MIT/Lincoln Laboratory; it is one of only two 8K×8K detectors yet incorporated into spectrographs (the other is in the IMACS<sup>4</sup> spectrograph for Magellan I). DEIMOS likewise has the first spectroscopic closed-loop flexure compensation system to come on line (other possible future units are in HROS<sup>5</sup> for Gemini South, GMOS for Gemini North, and IMACS for Magellan I).

The guiding principle of DEIMOS' design is minimizing contamination by bright terrestrial OH lines in the red spectral region. To achieve this, the design stresses two strategies: (1) relatively high spectral resolution to “get between” the OH lines and leave most of the spectrum OH-free, and (2) high flat-fielding accuracy to subtract the remaining OH lines to the limit allowed by photon statistics. The highest working spectral resolution in the red is  $R \sim 6000$  using a 1200-line grating, a dispersion of 0.33 Å per pixel, and a slit width of 0.75". Achieving high flat-fielding accuracy means holding the wavelength on each pixel constant (exactly how constant is stated below), and the closed-loop flexure compensation system (FCS) system was included for that purpose. Other goals are high throughput, long slit length for higher multiplexing, rapid slitmask alignment on the sky, speedy mechanism changes, and ease of use. The original design had a double-beam format with a total slit length on the sky of 33'. The second beam was deleted for cost reasons but could be restored if funding and demand warrant.

---

Further author information: (Send correspondence to S.M.F.)  
S.M.F.: E-mail: faber@ucolick.org; Telephone: 1 831 459 2944

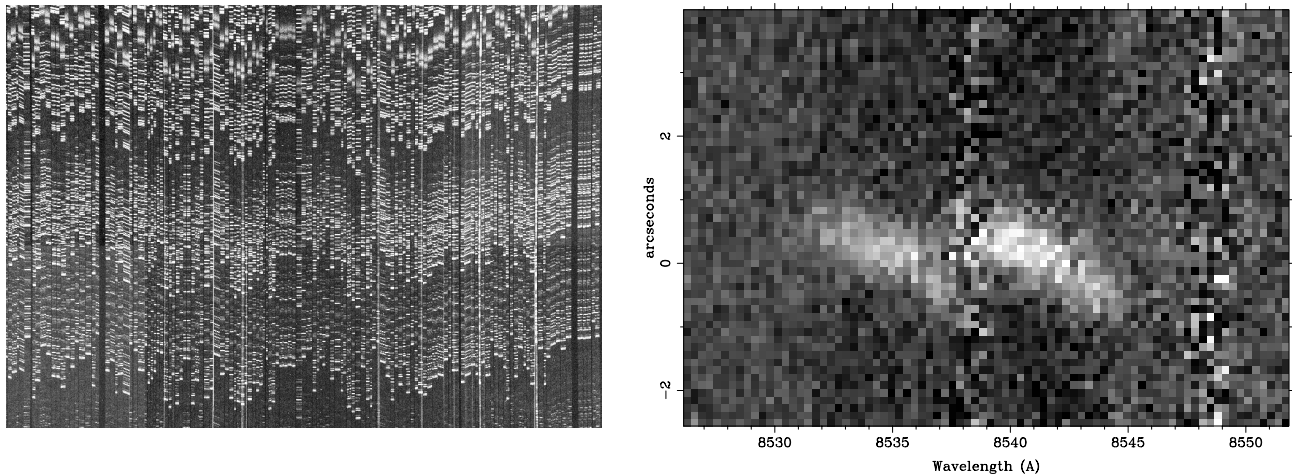


**Figure 1.** (a) Enlargement showing the upper 70% of a DEIMOS night-sky spectral image taken with the 1200-line grating. The wavelength range is roughly 7100 Å (bottom) to 8900 Å (top). The FWHM of the spectral lines is 4 px, or 1.3 Å. One hundred thirty-three slitlets are included in the mask. (b) Enlargement showing an [O II] 3727 Å rotation curve in a galaxy at redshift  $z = 1.29$ . The total velocity extent is about  $175 \text{ km/sec}^{-1}$ . Note that the noise under the subtracted night-sky lines appears to be random, as expected from photon statistics.

Fig. 1 shows sample spectra obtained during first-light commissioning in June 2002. A portion of a red multi-slit spectrum is shown in Fig. 1a, and an enlargement is shown in Fig. 1b. The spectra were taken at high resolution using the 1200-line grating. The enlargement shows a high-redshift galaxy at  $z = 1.29$  and illustrates the large amount of internal kinematic information available at this resolution.

DEIMOS was designed and constructed in the UCO/Lick Observatory Instrument Laboratories. Most of the work was done in-house except for the main structure, which was fabricated at L&F Industries, and the camera barrel, which was designed by Alan Schier and fabricated at Danco, San Jose. Major work started in the spring of 1994. The total project team numbered about 30 people, of whom 15 or so were typically focussed on DEIMOS at any one time. Initial funding for DEIMOS came from a Facilities and Instrumentation grant of \$1.79 million from the National Science Foundation (ARI92-14621). The California Association for Research in Astronomy (CARA) has contributed approximately \$7.2 million directly to the project, not including the additional costs of CARA liaison personnel and alterations to the Keck II telescope. UCO/Lick Observatory has contributed over \$1 million so far in manpower. A final cost accounting has not yet been done, but it appears that the total cost of the instrument, not counting the telescope alterations, will slightly exceed \$10 million.

The major optical and mechanical components are shown in Fig. 2. Light enters at left from the Keck II tertiary mirror through an open hatch and instrument window. The hatch area contains the TV guider, calibration light sources, and slitmask system. Slitmasks are thin sheets of aluminum housed in a cassette holding 11 masks at a time. An air-powered arm slides the masks onto a curved slitmask form, and constant pressure deforms them into a cylindrical shape that approximates the spherical focal plane to good accuracy.

After passing through the slitmask, light strikes an ellipsoidal collimator mirror, forming a 6-inch parallel beam. It is reflected back to a flat mirror dubbed the “tent mirror,” which, together with its unbuilt twin, diverts light to the sides to create the double-beam design. From there it travels to a 6×8-inch ruled grating (in spectroscopic mode) or a flat mirror (in direct-imaging mode). A linear grating transport system driven by a rotating lead screw carries three “sliders” holding two gratings and one mirror; the sliders are attached to Thompson ball bushings travelling on a rod. Each spectroscopic slider is provided with a friction tilt drive, and grating cells mount into the sliders using a combination of V-blocks and screw clamps.

From the grating/mirror, light enters the camera, which is the single most important element of DEIMOS. The state-of-the-art optical design is due to Harland Epps. Despite being highly refractive, the f/1.29 camera

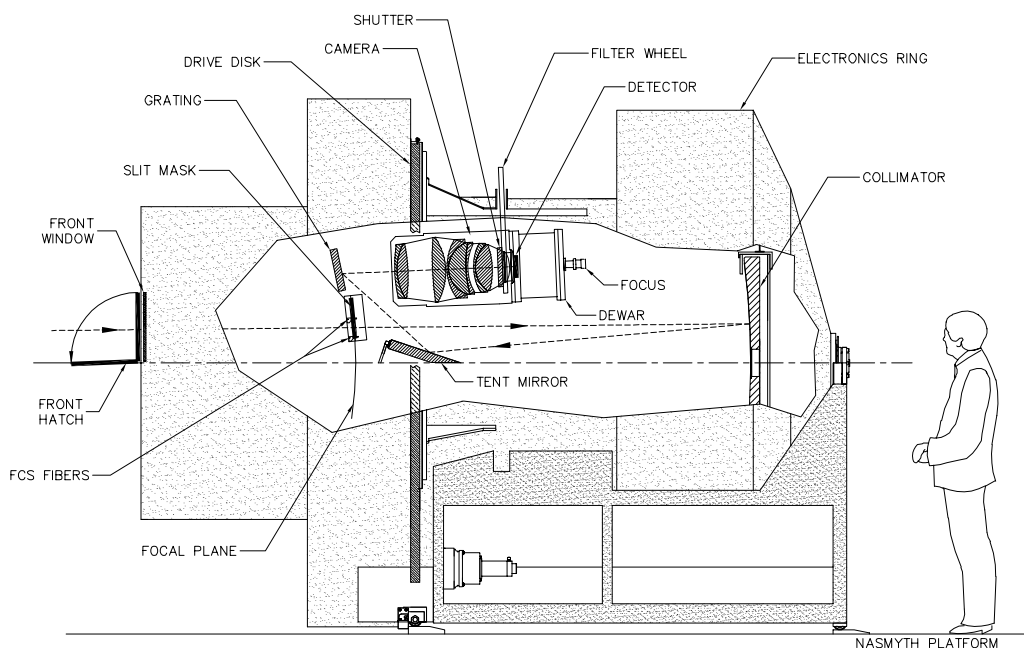


**Figure 2.** Light path and major optical components.

is nearly achromatic, both radially and axially, from  $4,000 \text{ \AA}$  to  $11,000 \text{ \AA}$ . However, the combination of steeply curved and highly aspheric surfaces imposes extremely tight tolerances for fabrication and assembly. The camera is temperature-sensitive and images differently when tested at room temperature than at the operating temperature of  $0 \text{ C}$ . The plate scale also varies with temperature and must be appropriately compensated. Fluid coupling of the doublets and multiplets adds to the mechanical complexity. The lenses are radially supported by athermalized RTV mounts, and these, together with the coupling fluid and other components, posed significant materials incompatibility issues.

Fig. 3 shows the camera, shutter, filter wheel, field flattener, dewar window, and detector. A critical dimension for camera performance is the axial spacing between the last optic in the camera and the field flattener; errors as small as  $0.005\text{-inch}$  in this parameter generate detectable radial coma. Also shown is the thermal compensator, which passively adjusts the axial location of Multiplet 4 to maintain constant plate scale versus temperature. Lastly (not shown) is a pair of lateral X-Y adjusting screws on Multiplet 4 built into the cell to compensate for lateral coma caused by assembly errors such as tip-tilt and decentration. The recommended assembly tolerances for the camera were  $0.001\text{-inch}$  in every dimension; these were considered to be so tight that the lateral adjustment was included as insurance, which proved very useful (see below).

The layout of the mosaic detector is shown in Fig. 4. The detector consists of 8  $2048 \times 4096$  CCDs fabricated by MIT/Lincoln Laboratories. Two separate mosaic detectors were actually built, an early one comprised of blue-sensitive CCDs, and a later one of red-sensitive CCDs. The red CCDs have a high-resistivity epitaxial layer that is  $45\mu$  thick, more than twice the typical  $20\mu$  thickness of the blue-sensitive CCDs. Their QE is 23% at  $10,000 \text{ \AA}$ , roughly 2.5 times higher than the blue CCDs. Both types were developed under the leadership of Gerry Luppino, who coordinated the consortium partners funding the production runs, and Barry Burke, who leads the MIT/Lincoln CCD group. Fringing on the red CCDs is exceptionally low, with fringe amplitudes in the far red of only  $\pm 2\%$ . Even so, with a fringe-wrap cycle length of  $24 \text{ \AA}$ , the goal of  $0.2\%$  rms flatfielding accuracy implies a wavelength stability of only  $0.4 \text{ \AA}$  rms on each pixel, or  $0.6 \text{ px}$  rms with the 600-line grating.

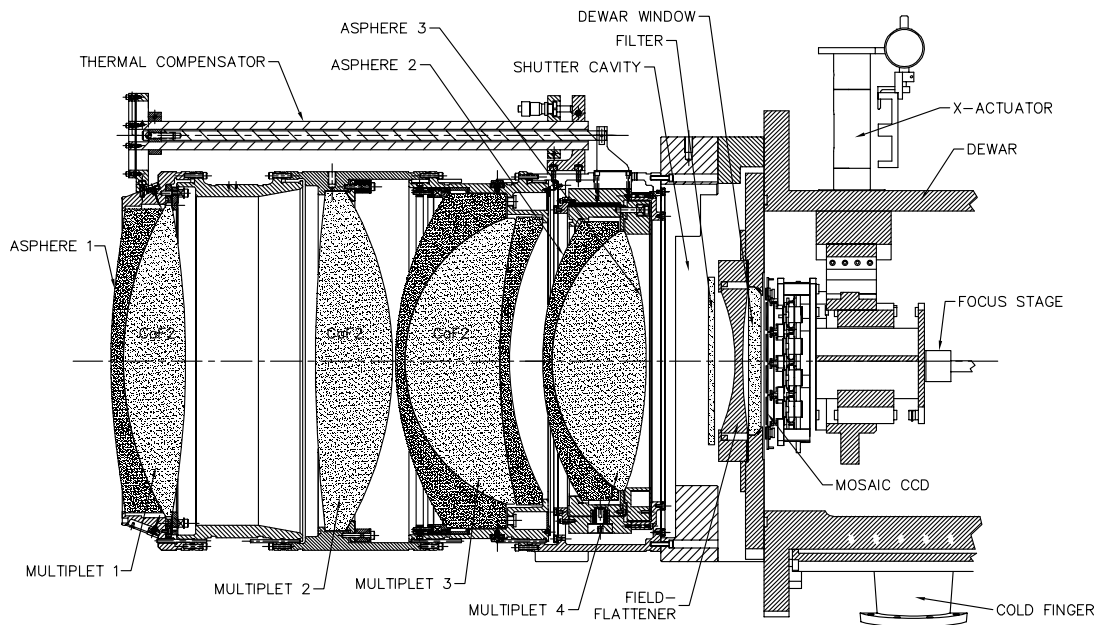


**Figure 3.** The camera optics, camera cell, shutter, filter wheel, field flattener, dewar window and detector.

Flanking the main science CCDs in Fig. 4 are two smaller  $600 \times 1200$  CCDs belonging to the flexure compensation system (FCS). The FCS CCDs receive images of 4 optical fibers positioned in the focal plane, two at either end of the slitmask form (see Fig. 2). Light is fed through these fibers from a CuAr lamp (in spectroscopic mode) or a white LED (in imaging mode). One of these sources is continuously on, and images from the FCS CCDs are constantly read out every 15 seconds whenever the shutter is open. It is abundantly clear that the FCS system is essential to normal operations; the amplitudes of the uncorrected image motions are large, but the FCS system manages to reduce them to tolerable levels. More details are given below and in the paper by Kibrick et al.<sup>6</sup> in these Proceedings.

The last major system in DEIMOS is the rotation system. This also had to be built to higher standards because DEIMOS' slit length is over twice as long as previous Keck instruments, necessitating twice the accuracy in position angle. As we elected not to include a TV guide camera at the periphery of the field, the responsibility for maintaining PA rests solely with the rotation system, which is working blind. Strategies used to test the absolute accuracy of the rotation system before going to the telescope are described below. More details on the rotation system may be found in the paper by Deich et al.<sup>7</sup> in these Proceedings.

In addition to the above challenges, three others can be added. (1) As instruments get larger, flexure affects not just the optics but all major mechanical systems, disturbing the relationship of subcomponents. Prime examples in DEIMOS are the grating system and the slitmask system, in both of which components are handed off from a storage/transport system to a mount. Getting these stages to work took much more time than expected because of flexure. (2) Observers using multi-object spectrographs should be able to expect to use the same slitmask with any grating in any slider. Spectral positioning along the slit should therefore be the same with all grating/slider combinations or else effective slit length will be lost. Additional slit loss is caused by misalignments between the spectral direction and the columns of the detector. Both kinds of losses are exacerbated by the presence of gaps in the detector along the slit direction. Our detector has four CCDs along the slit direction, and therefore slit-length losses occur at four edges, not just one. To keep slit-length losses under control requires mounting all gratings in cells in exactly the same way, mounting cells in sliders similarly, and ensuring that all sliders clamp up the same way regardless of gravity. This optical alignment program was

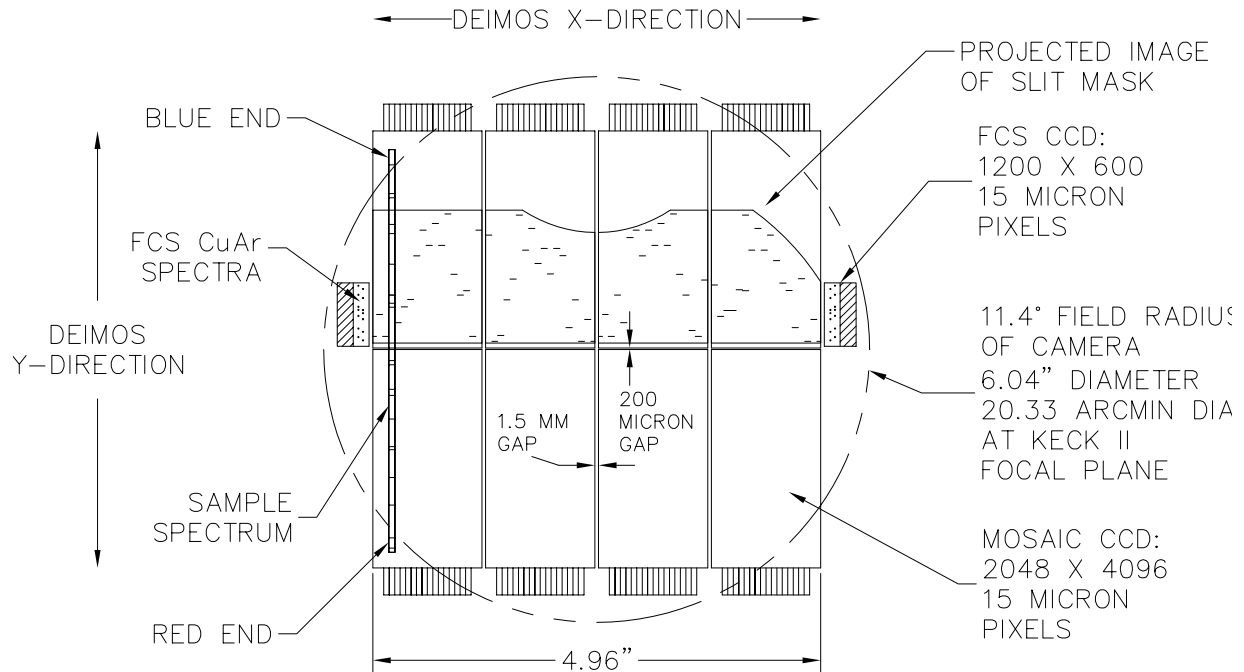


**Figure 4.** The detector focal plane showing the 8 2k×4k science CCDs, the two flanking FCS CCDs, and an overlay of the direct-imaging field of view.

surprisingly time-consuming, and in fact it is still not quite completed. (3) The third challenge is the increasing dependency on complex software for even basic operations. The flexure compensation system on DEIMOS is one example; the spectrograph cannot work without it, yet the software contains many elements that we had never dealt with before. A second example is the slitmask environment, which was planned from at the start to be a seamless system that included mask design, mask database creation, mask fabrication, mask installation and verification, mask alignment on the sky, and final data reduction. Key software components are involved at each step that must interface well with one another and with their relevant mechanical partners. Each stage of our slitmask system has now been exercised at some level, but we cannot yet claim to have a smoothly working system (see Clarke et al.<sup>8</sup> in these Proceedings). The amount of planning and training for observatory staff to operate one of these complicated systems is also substantial.

## 2. OPTICAL ASSEMBLY AND TESTING

The remainder of this paper explores the above challenges in more detail. Two large sections focus on the major problems of image quality and image motion, while a third section is devoted to items that went well. The emphasis is on highlighting problems that proved to be more difficult than originally expected and strategies that were developed to deal with them.

The collimator and camera elements were polished in the UCO/Lick Optical Shop. We had previous experience in making difficult aspheres (e.g., the f/15 secondaries for the Keck I and Keck II telescopes and the aspheres in the LRIS camera) and had developed a profilometer system for testing them. Optical fabrication went smoothly except for a small crack that spontaneously appeared at the edge of one CaF<sub>2</sub> element. As procuring the CaF<sub>2</sub> blanks had been *extremely* difficult, we gambled and hoped that the crack did not worsen. So far the gamble has paid off. One of the aspheres was also broken at the coating company and had to be completely redone.

Several different materials coexist in the camera. These include the optical coupling fluid (LL1074 from Cargille), mylar spacers used to space the multiplsets, O-rings used to seal the fluid gaps, bagging and tubing



**Figure 5.** Final assembly of the camera on its rotating turntable.

used for the fluid reservoirs, RTV used to dam the fluid, and finally the optical glasses. Although the fluid was claimed to be relatively inert, to be safe we tested it in conjunction with other candidate materials in a year-long testing program<sup>9</sup>. This uncovered significant reactivities among several of the proposed components and led to major changes in materials choices.

The camera fabrication and assembly tolerances were determined by Mike Rodgers of Optical Research Associates using their Code V tolerancing package. As noted, the final tolerances amounted to 0.001-inch in every dimension. The optical elements therefore had to be centered and leveled in their cells to better than this, and the cells had to be put together to similar accuracy. Fortunately, the steel camera cells were well machined by Danco and went together fairly easily. The crucial tools used to complete the assembly were an accurate rotating table and a last-word gauge (see Fig. 5). These were used in combination to measure the runout of each surface and the azimuth of maximum deviation; an Excel spreadsheet told us immediately how to correct. Accuracies repeatable to about 0.0005-inch were achieved. Reference surfaces, both axial and radial, were machined into the outer surfaces of the camera cells to serve as guides for mounting the lenses and for assembling the cells into the final camera. As handling the camera elements was risky, each stage of the assembly process was scripted in advance; the final script for the whole camera contained over 1000 separate steps.

The aberrations of the optical design were sufficiently large that we could not learn much from interferometric tests, and the major test data came instead from optical images. A major impediment to camera testing was the lack of a capable detector to cover the whole 6-inch field. That would not be available until the camera was in the spectrograph with the main detector. Initial tests in the optical shop were accordingly rather brief and limited to verifying the correct back focal distance (approximately) and quickly assessing optical quality. A small CCD detector (Cohu TV camera) was used in conjunction with a microscope to sample the images. This setup was far from ideal: the field of view was tiny (0.5 mm by 0.7 mm), the Cohu had limited dynamic range making faint portions of the PSF hard to detect, and it was difficult to focus off axis. Later, after optical problems arose, we managed to devise several useful optical tests that could in fact be conducted in the lab with the Cohu alone. We probably could have saved time overall had we spent more time testing the camera (and its separate multiplets) early, before putting the camera into the spectrograph.

The first images in the spectrograph revealed large radial comatic tails plus considerable lateral coma. Tails ranged in length from 17 pixels on the red side to 12 pixels on the blue side. Fortunately we had a few representative spot diagrams at room temperature from ORA, and these showed radial comatic tails of about



one-half the observed length, suggesting that a considerable fraction of the radial coma would resolve naturally at 0 C, the nominal operating temperature. Further modeling with Zemax suggested that an additional source of radial coma might be an error in the spacing between the back of the camera and the field flattener. When the camera was later disassembled for shipping, we found that a spacer there had indeed been omitted.

Regardless of the source of radial coma, the Zemax tests suggested that modulating the final element spacing would be a good way to tune it out. We might have tried this during testing but were prevented from doing so by another error in which the detector was placed a little too far back in the dewar. This was exacerbated by small changes to the dewar window support structure, which moved it a little forward. Moreover, we found later that the dewar front plate bowed *out* over the O-ring seal slightly when tightened, and that the detector support structure also moved *down* in the dewar when vacuum was applied. Finally, the spacings in the triplet (Multiplet 3) proved to be a little too thick. Although each of these five effects was individually small, they all conspired in the same direction to place the detector too far from focus. As a result, we never went fully through focus during testing, and the proposed increase to the spacing between Multiplet 4 and the field flattener would have made matters worse.

These effects were discovered in a systematic remeasurement program during teardown for shipping to Hawaii, and the detector was moved almost 2 mm forward in the dewar as a result. In addition, we were urged by the Preship Review Committee to test the camera alone on the dome floor at the operating temperature before installing it in the spectrograph. We did this using the Cohu, and, to the limits allowed by that little detector, verified that the camera made good images after the spacing between Multiplet 4 and the field flattener was properly adjusted. Final optical tuning in the spectrograph utilized both direct and spectroscopic images over the whole science detector, with slightly higher weight given to spectroscopy. The spacing between Multiplet 4 and the field flattener received a final tweak, and the X,Y screws on Multiplet 4 were adjusted to remove the last vestiges of lateral coma. The detector focal plane tilt was also adjusted by varying the three shims used to space Multiplet 4 from the field flattener.

The resultant images (through 0.5 arcsec pinholes in spectroscopic mode) now vary in width from 1.3 px at field center to 1.5 px at the edges ( $1-d \sigma$ ). Images are round over virtually the whole field of view. These images are very good but do not quite approach the predicted sizes based on the known design and fabrication errors, which range from 1.0 px at field center to 1.3 px at the edge of the field ( $1-d \sigma$ ). This effect was actually discovered during testing in Santa Cruz by measuring image sizes with a beam stopped down so far that design and assembly errors were negligible. The best images then were also about 1.1-1.3 px, similar to the best images we see now through a much bigger pupil. At that time we suspected image broadening due to charge diffusion in the CCDs. However, Shack-Hartmann testing of the camera before shipping revealed a pattern of random, small-scale wavefront errors; this pattern was also seen as brightness fluctuations in images far from focus. None of the camera polishing techniques is known to be capable of producing such a pattern—the spherical surfaces should be locally quite smooth, and errors on the aspheric surfaces should be azimuthally symmetric, not random. Our best guess now is index of refraction inhomogeneities in the CaF<sub>2</sub>, as DEIMOS has perhaps the longest path length yet of CaF<sub>2</sub> in an astronomical camera. Inspection of all three CaF<sub>2</sub> elements under crossed polaroids after polishing did indeed show significant wavefront *differences* between polarizations across each element of about 1 radian rms, including a lot of very fine-scale structure. However, no attempt was made to measure any *absolute* wavefront errors at that time.

Several lessons emerged from building the DEIMOS camera: (1) An accurate rotating table is an absolute necessity; ours cost several tens of thousands of dollars but it was worth it. (2) Mechanical adjustments should be included if at all possible to counteract low-order aberrations. In our case, the adjustable shims between Multiplet 4 and the field flattener could correct any radial coma (as might come from errors in the aspheric surfaces, for example), and the lateral X,Y adjustment of Multiplet 4 could correct lateral coma caused by tilts or decenterings of the lenses. Later measurements did indeed show that Multiplet 4 had mysteriously moved laterally out of position by about 0.003-inch, possibly because its RTV radial support cured asymmetrically. Some stackup tilt error also crept in during camera assembly because the individual multiplet cells departed slightly from being plane parallel all in the same sense. If we had not had a lateral coma adjustment, these errors would have caused noticeable image degradation even though overall we met (and in fact exceeded) nearly all the assembly tolerances. (3) A large detector should be procured for optical testing with good dynamic range.

If it is not physically large enough to cover the whole field of view, a precision stage should be built to move it around accurately in the focal plane. (4) A broad set of spot diagrams or other diagnostics should be available at the testing temperature as well as the final operating temperature. (5) The camera multipliers should be characterized fully before assembling them into the final camera and before the camera is put into the spectrograph. Measurements should include a final check of the tilts and decenters of all accessible surfaces, the thicknesses of all multipliers and their spacings, and a precision measurement of back focal distance of the assembled camera.

### 3. FLEXURE AND IMAGE MOTION

The original specification on image motion called for a limit of 0.25 px rms (averaged across the detector within a single exposure) between an evening observation and its afternoon flat field. This specification was set for two reasons: to maintain image quality, and to achieve a flat-fielding accuracy of better than 0.2% for photon-limited sky subtraction with the 600-line grating. The flat-fielding specification was later relaxed by a factor of two when the actual fringing behavior of the red CCDs became known (see above).

It was deemed unlikely that we could build such a rigid structure without some form of flexure compensation. We had had no experience with open-loop correction systems (such as was later used successfully on the ESI spectrograph), and in any case the flexure actually observed on DEIMOS has enough hysteresis that an open-loop system by itself would not work anyway. Accordingly a closed-loop, fully independent flexure compensation system (FCS) with separate light sources, detectors, and signal chain was designed in from the beginning.

The FCS system is more fully described by Kibrick et al.<sup>6</sup> in these Proceedings. It has two actuators: a linear motorized X-stage in the dewar that moves the detector laterally along the slit direction, and a piezo-electric Y-actuator that tilts the tent mirror and moves the image along the spectral direction. These correct any image motions coming from the same mechanical motions to high accuracy. However, the correction of other motions is not perfect in spectroscopy mode, since gratings, unlike mirrors, produce geometric distortions. In our system, it turns out that all Y-motions are fairly correctable but that X-motions are only partially correctable (leaving residual distortion errors of 5-10%). Thus, it is particularly important that X-motions be kept small.

In addition, the system is completely unable to correct image rotation or plate-scale changes. Rotation in DEIMOS comes mainly from a sag of the tent mirror about the optical axis, and the mount has to be sufficiently rigid to prevent this. Plate scale changes come from focus changes and from camera temperature changes, and a passive thermal compensator was built into the camera that alters the spacing between Multipliers 3 and 4 with temperature to take out the latter effect (see Fig. 3). Yet a third limitation is set by the travel of the FC actuators. In our case, the X-actuator moves the image by only about 26.4 px, and the Y-piezo moves it by only 23 px (which is further reduced to 12.9 px with the 1200-line grating by anamorphic demagnification at its reddest tilt).

Results on first assembly showed a total image motion under rotation of about 40 pixels pk-pk in X and 7 pixels pk-pk in Y. The X motion was especially dangerous because it far exceeded the range of the X-actuator and because X motions are inherently less correctable. There ensued a long campaign to find the sources of this flexure and remove them. Some of the techniques used were familiar: place dial gauges and Mahr gauges on parts, add extra braces and temporary clamps, perform FEA analyses, remove individual parts and place them on a separate rotation test stand, etc. Lateral motion of the collimator was measured by viewing a centrally mounted cross-hair through an alignment telescope along the optical axis. I mention here three more methods that were developed especially for DEIMOS.

(1) Camera double-pass test: a small optical fiber was rigidly mounted in the center of the camera focal plane next to the Cohu detector. Light passed from the fiber out through the camera, struck a mirror mounted to the camera mouth, traveled back into the camera, and formed an image on the Cohu. The position of this image was sensitive to variable decentrations of the camera elements and variable wedge in the camera multipliers. Testing at disassembly before shipping showed that Element 3 was in fact loose and also that significant wedge was being created by the hydrostatic pressure head from the coupling fluid interacting with compliance in some of the axial lens supports. In certain double-pass tests, the mirror was also moved to the grating support

structure, where it could be used to measure flexure in the hard points on which the gratings were mounted. The double-pass test needs only the camera and was later used extensively in the optical lab before shipping.

(2) Camera pinhole test: a pinhole light source was rigidly mounted to the front of the camera to uniformly illuminate all optical elements. Small bubbles in the fluid and dust particles on the optical elements cast shadows onto the science detector. The axial location of each particle was determined by moving the pinhole laterally a known amount and observing the transverse motion of its shadow; particles on surfaces closer to the pinhole moved more. The motions of all shadows were then clocked as DEIMOS rotated. This test was particularly valuable as it measured the transverse sags of optical elements individually, not cumulatively as in test (1). It also measured the transverse sag of the detector relative to the dewar window, which was found to be small. This test likewise did not need the spectrograph and was repeated in the optics lab before shipping.

(3) General optical model: an optical model of the entire light path was used to perturb the positions of optical elements and determine the effects on spot locations. Individual elements, or groups of elements, have specific distortions, and thus signatures. From test images taken at different position angles, it was possible to deduce what was moving. This was enhanced by taking long exposures containing ghost images due to reflections off the detector and again off the grating in zeroth order, when the grating is face-on to the camera. These acted like a variant of the double-pass camera test described in (1) above and were a powerful probe of grating motions in particular.

The results of these tests traced the largest single source of flexure to the grating support structure, a steel box composed of plates fastened with screws. The baseplate of this box was thickened, more screws and plates were added, and the mounting to the drive disk was tightened. The second-largest source of motion was in the camera due to decentration of Element 3, whose radial shims were loose, and to the variable wedge caused by hydrostatic pressure. Separate work on the camera prior to shipping reduced image motion from these causes from 10 px down to 3 px. Based on an FEA study, some stiffening was also added to the grating sliders.

It was predicted from the optical model that some of these sources of image motion were cancelling one another in Y (the spectral direction), and that reducing the X motion would act to increase the Y motion. This prediction was confirmed during commissioning. Our present image motion is 8 px in X (pk-pk) but 18-23 px in Y (depending on the slider). The motion in X is now well within the correctable range of the FC system, but the range in Y, though geometrically correctable, exceeds the range of the piezo actuator on the tent mirror, at least for high dispersion gratings with large anamorphic factors. The present scheme therefore uses the grating tilt for coarse motions and the tent mirror for fine motions. We are still analyzing the source of the remaining image motion and believe that it comes mainly from the grating system, probably the sliders.

Our testing of the FC correction accuracy is only partially complete (see Kibrick et al.<sup>6</sup>). Two recent hour-long sequences of four spectra each were FCS-corrected using just one spot on one of the FCS detectors. Shear was seen in Y varying along the X direction, together with an overall rotation of the image. Total motions over a rotation of 56° were roughly 0.5 px rms averaged over the whole science detector. We estimate that these would be reduced to 0.3 px rms if correction signals from both FCS detectors had been used. This compares favorably to our motion goal of 0.6 px rms, but we still have not yet fully tested motions between afternoon flat-fields and nighttime exposures, and it is likely that these will be larger than the motions within single images. However, given present information, we are optimistic that the total image motion over all PAs will meet our specifications once the system is fully operational.

It appears from experience gained with DEIMOS and other recent large astronomical instruments that flexure is inevitable in such instruments if they change orientation with respect to gravity. Nearly all recent instruments have had it, and the problem will only grow worse as telescope size increases in the future. It is best to anticipate flexure and build solutions in from the beginning.

In our case, the flexure from the main structure was fairly easy to analyze and keep small—it was flexure in the subsystems that was troublesome. Most such subsystems have complicated internal articulations that are not easy to analyze using FEA. They are also more likely to exhibit hysteresis, which vitiates open-loop correction. Finally, flexure can threaten the very operation of systems that involve internal hand-offs; it can be so severe that the parts simply do not mesh. That problem occurred in both major hand-off systems on

DEIMOS—between the slitmask cassette and slitmask form, and between the grating transport system and the grating mount. Extensive stiffenings of these systems were needed to get them to work.

It would have been good to have found and corrected these problems earlier. We opted to use the spectrograph as our main rotating test stand, and access both in time and space was tight at the end of the project when several systems needed attention at once. In retrospect, we should have approached the problem of flexure more aggressively by *assuming* that it would be present in every subsystem, designing systems more modularly, including ways in which flexure could be measured (such as mounting points for test equipment), building more prototypes, and testing them more thoroughly on a capable rotating test stand. This mindset would have saved time in the end.

A key tool in finding flexure was a series of software scripts that ran robotically overnight. These scripts recorded a wide range of parameters, including encoder positions, alarms, and image locations on both the FCS detectors and the science detectors. The FCS system proved to be particularly convenient for image-motion measurements as its images were small and it was often working even when the science detector was not. The imaging data were so voluminous that a separate software person had to be hired part-time to analyze them. These automated scripts collected thousands of data points at all position angles and gave us a definitive view of flexure in the system. We are still using these scripts to debug the FCS system.

#### 4. SUCCESSES

We conclude with a brief review of things that went well and strategies that worked.

In this category we place the mosaic detector and associated electronics. The detector signal chain is described in more detail by Wright et al.<sup>10</sup> in these Proceedings. We would like to take this opportunity to thank the MIT/Lincoln team and Gerry Luppino for making our CCDs; they are almost perfect. One amplifier connection on CCD5 is not working, which forces us to read the whole array in single-amp mode. The readout time for the whole array is thereby slowed from the goal of 39 sec to 70 sec, but we hope to recoup most of that soon by revamping the way that data bits are streamed onto the optical fiber video connections. CCD5 is also affected by cross-talk (up to 2 DN in amplitude) from its neighbor CCD6, and we suspect that a broken wire is acting as an antenna and picking up stray radiation (which may also explain the dead amplifier). This is a candidate for repair the next time we open the dewar; in the meantime, we can remove the cross-talk to an accuracy of about 0.5 DN or better by scaling and subtracting the signal on CCD6.

The CCD electronics were provided by Prof. Bob Leach of San Diego State University (Leach II controllers). The video cross-talk between the A and B amplifiers on the same board is currently 1 part in 20,000. That would pose an annoyance if we were reading out in dual-amp mode, but our present plan to use single-amp mode sidesteps the issue. Aside from that problem, the boards have worked well. More spares would have been handy for diagnostic purposes.

The UCO/Lick CCD Laboratory tested all the CCDs coming from the MIT/Lincoln consortium runs, some 100 in all, a huge task. Given their experience in handling CCDs, lab personnel also did all the metrology on the CCDs and installed the final CCDs on the mosaic. At one time we considered using various elaborate fixtures and jigs to place the CCDs, but eventually we relied on simple hand placement. CCD heights were measured with a microscope custom-fitted with an X,Y,Z stage and were mounted on molybdenum blocks designed by Gerry Luppino; to level the CCDs, pad heights on the blocks were shaved to  $5\mu$  accuracy using a CNC mill.

The job of placing CCDs on the backplane was complicated by the fact that the silicon actually overhung the edges of the aluminum nitride packages by several tens of microns in some cases, making accidental bumping very risky. Accordingly, we installed safety bumpers on the backplane along the short sides to prevent pairs of CCDs from touching in that direction. The resulting spectral gaps are 12-21 px ( $180\text{-}330\mu$ ). The pixel gaps along the long sides average 1.5 mm and do not require bumpers. The CCDs were positioned on the backplane in this direction by lining up the first one against a pair of longitudinal bumpers and placing succeeding CCDs in X by using a standard spacer to set the width of the wide gaps. The final rotation of each CCD was tweaked by aligning to its neighbor by eye under low magnification. This technique succeeded in orienting each CCD to within 10 px along its length of 4096 px.

We were fortunate in having two fully operational CCD mosaics, plus an engineering mosaic of partially functioning devices to debug the electronics. Despite intense planning, we still had multiple troubles with our power-up and power-down cycles, and software and hardware control of these cycles had to be reconfigured several times. There was even some disagreement as to the proper power-down procedure for the MIT/Lincoln CCDs (see Wright et al.<sup>10</sup> these Proceedings). External power failures during testing were common and stressed the system several times. We actually lost two engineering CCDs during testing, at least one of which was likely due to an improper power-failure procedure. By the time the precious red mosaic was installed in the dewar, it was reassuring to know that all of these bugs had been worked out. It is hard to imagine how we could have tested all the electronics without having a complete spare engineering mosaic.

As mentioned, spectral alignment is more critical in multi-slit spectrographs with mosaic detectors, as effective slit length can be lost through a variety of spectral misalignments at each CCD gap. To mount all gratings in their cells the same way, we designed an alignment jig that holds a laser in a fixed position. The laser shines on the grating and reflects off to a target about 40 feet away. A grating in its cell is held with the same trunions that hold it in the spectrograph and is rotated through multiple orders, typically 7. One grating was adopted as standard, and all others were adjusted to it. The grating to be adjusted was adjusted in its cell so that the spots from all orders fell in the same place and the absolute location on the target matched that of the standard grating. This technique worked fairly well, and the spectral orientations and positions along the slit of all gratings match to within about 20 pixels. With these and other adjustments, we succeeded in reducing the total slit loss to about 300 px, or 3%. Of this, about 100 px is due to spectral curvature and cannot be avoided.

Apart from some early connector problems, the TV guider and associated optics have been relatively trouble-free. The TV camera consists of a 200-mm Canon lens feeding a 1024×1024 Site CCD in a PXL camera. The camera stares directly at the focal plane with a 3.5×3.5 arcmin field of view; there are no moving stages. Roughly one third of the field is a rectangular pickoff mirror with a curved surface to maximize light through the Canon lens. The other two-thirds lies on the slitmask, which is also moderately reflective. To compensate for TV flexure, we placed 6 reseau marks on the pickoff mirror and intended to guide relative to them, not the TV pixels. However, the sky illumination proved to be too faint to show these marks, and we have fallen back to open-loop flexure correction, which is accurate to ±0.5 px, or 0.1 arcsec. The reseau marks are visible with the calibration lamps turned on, however, and are very handy for measuring flexure.

DEIMOS' rotation is driven through a friction drive acting on the periphery of the drive disk (see Fig. 2). The specification on accuracy is 17" rms, which corresponds to 0.05" rms on the sky at the ends of the slit, or about 0.004 inches at the edge of the drive disk. Two Renishaw optical encoders read a precision tape stretched around a disk mounted on the rear bearing. The two read heads are about 131° apart. The drive is supposed to be able to track within 0.5° of zenith, at which point the rotation speed is about 0.7° per second. More details on this system can be found in the paper by Deich et al. in these Proceedings.

As servo-loop parameters for the rotation system were being tuned, dynamic tests were conducted in which a computer program simulated tracking demands from the Keck drive-and-control system. Satisfactory tracking was achieved in which the encoder errors were almost always below the specified limit except for very brief periods near the zenith. Absolute accuracy was tested in the lab in two ways. A laser was attached to the main barrel, and DEIMOS was rotated through angles up to 720° forward and back. This established the number of counts per rotation and showed that backlash and hysteresis were negligible. The single remaining issue was linearity. We tested this roughly in the lab by mounting a gauge block to the rear of the drive disk and placing a level on one face. DEIMOS was rotated to level this level, and the encoder count was recorded. We rotated 180°, releveled the level, and recorded the encoder again. The block was then moved around the periphery of the drive disk in 30° steps, and the process was repeated. If the rotation encoder is perfectly linear, all encoder differences will be the same. This test can uncover errors of the form  $\cos \theta$  but not error terms of  $\cos 2\theta$  and higher.

The results were quite interesting. A  $\cos \theta$  term with half-amplitude 15" was detected in the *average* reading of the two encoders. However, the error in each encoder separately had an amplitude of 500", far larger than the allowed specification. We can account for the data if we imagine a small motion of the center of the disk

holding the Renishaw tape as DEIMOS rotates. If the Renishaw heads were exactly  $180^\circ$  apart, this error would completely cancel; as it is, it cancels to within about 7%. We have now included a  $\cos \theta$  correction term to both encoders and use the average of both to keep the maximum error small.

Star-trail measurements have been taken at multiple position angles on the sky to study terms of the form  $\cos 2\theta$  and higher, and these data are still being reduced. However, we have also taken direct images while tracking to within  $0.7^\circ$  of zenith, and the images look round. It appears that the rotation system is performing well.

We close with a brief description of the automated system of test suites that was developed for DEIMOS. This “ktest” software<sup>11</sup> was originally developed for ESI and was easily adapted to DEIMOS. However, DEIMOS presented several features that rendered its test program more complicated. An enormous advantage of DEIMOS is that its rotator is part of the instrument. Once the rotator was operational, all stages could be tested at various gravity vectors. But this advantage was also a complication, as each test suite suddenly became 5 test suites needing to be run at  $0, 90, 180, 270,$  and  $360^\circ$ . The volume of data ballooned enormously, and the amount of time needed to complete the tests on the instrument expanded accordingly.

As noted above, DEIMOS also had two particularly complex stages, both of which incorporated two or more independent actuator systems into an apparent single device. The slitmask “stage” was really a scissors jack driving a storage cassette and a separate pneumatic arm pushing masks into place. The grating “stage” was really a linear drive bringing gratings to the light path, plus a set of pneumatic clamps locating the selected grating in place once it arrived, plus an independent tilt mechanism for each grating which could be operated at any time (whether selected or not, and whether the linear stage was in motion or not).

Both of these stages involved elaborate state and limit sensing, and both were subject to flexure and resistance varying with the gravity vector. A significant amount of custom test code had to be written to test them. Software staff estimate that more than half of the total testing effort went into these two stages. The existing “ktest” suite sufficed for most other stages and, to some extent, for the individual components of these compound stages, tested in isolation.

As a result, testing for DEIMOS separated into two parallel efforts. The standard “regression testing” activity using individual actuator tests continued much as it had for ESI, but with new, higher-level, more “condensed” data reduction to produce a shorter and more easily understood report. Testing of the problematic compound stages proceeded mostly under manual control and involved automatic collection of hundreds of FCS and science images. As noted, these were used to assess flexure of the instrument as a whole and the effect of gravity on the critical grating clamping and tilt mechanisms. During the last 6 months of the instrument’s time on the mainland, most stages were subjected to several thousand individual pass/fail tests.

## ACKNOWLEDGMENTS

Financial support of DEIMOS from the National Science Foundation, the California Association for Research in Astronomy, and UCO/Lick Observatory has already been acknowledged. We would like to take this opportunity to recognize Harland Epps for his superb optical design for DEIMOS, which is the foundation on which the instrument is built. Brian Sutin designed the collimator, did an influential early tolerance analysis of the camera elements, and finalized the optical layout of the TV camera. Mike Rodgers of ORA did the final tolerance analysis and was an invaluable resource in addressing many questions that came up during camera construction.

DEIMOS’ CCDs were provided by the MIT/Lincoln Laboratory in collaboration with Gerry Luppino of the University of Hawaii. We thank Terry Mast of the UCO/Lick staff for his intense early involvement in DEIMOS and, most especially for his seminal contributions to camera and mosaic assembly. In addition, we gratefully mention the superb cooperation we have had from the CARA staff at all levels during the complex transfer of DEIMOS from the UCO/Lick Shops to Keck Observatory. This transfer has required extensive modifications to both hardware and software at Keck and, indeed, is still going on. The Observing Assistants of the Keck II telescope are to be praised for rendering superb service at a time when the instrument behavior was not yet fully predictable. We also thank members of the DEEP Survey team, notably Ben Weiner, who provided

an illustration for this paper, and Doug Finkbeiner, whose development of a timely DEIMOS data reduction pipeline for multi-object spectra has added greatly to our early understanding of instrument performance. We also acknowledge the excellent advice we received from our outside review committees, especially from Dan Fabricant; Dan chaired several of our committees and provided encouragement and key suggestions throughout the project.

Finally the authors wish to recognize and acknowledge the very significant cultural role and reverence that the summit of Mauna Kea has always had within the indigenous Hawaiian community. We are most fortunate to have had the opportunity to work there and conduct observations from this very special mountain.

## REFERENCES

1. D. J. Cowley, S. M. Faber, D. F. Hilyard, E. C. James, and J. Osborne, "DEIMOS: A wide-field faint-object spectrograph," in *Optical Telescopes of Today and Tomorrow*, L. Ardeberg, ed., *Proc. SPIE* **2871**, pp. 1107–1115, 1997.
2. E. C. James, D. J. Cowley, S. M. Faber, D. F. Hilyard, and J. Osborne, "Design update of DEIMOS: A wide-field faint-object spectrograph," in *Optical Astronomical Instrumentation*, S. D'Odorico, ed., *Proc. SPIE* **3355**, pp. 70–80, 1998.
3. M. Davis, and S. M. Faber, "The DEIMOS spectrograph and a planned DEEP redshift survey on the Keck-II telescope," in *Wide Field Surveys in Cosmology*, S. Colombi, Y. Mellier, and B. Raban, eds., p. 333, Editions Frontieres, Paris, 1998.
4. B. C. Bigelow, A. M. Dressler, S. A. Shectman, and H. W. Epps, "IMACS: the multiobject spectrograph and imager for the Magellan I telescope," in *Optical Astronomical Instrumentation*, S. D'Odorico, ed., *Proc. SPIE* **3355**, pp. 225–231, 1998.
5. P. D'Arrigo, R. G. Bingham, A. Charalambous, K. Saber-Sheikh, and T. E. Savidge, "Active flexure compensation for the HROS spectrograph," in *Optical and IR Telescope Instrumentation and Detectors*, M. Iye and A. F. Moorwood, eds., *Proc. SPIE* **4008**, pp. 861–865, 2000.
6. R. I. Kibrick et al., "A comparison of open versus closed loop flexure compensation systems for two Keck optical imaging spectrographs: ESI and DEIMOS," in *Instrument Design and Performance for Optical/Infrared Ground-Based Telescopes*, *Proc. SPIE* **4841**, 2002.
7. W. T. S. Deich, R. I. Kibrick, S. M. Faber, D. A. Clarke, and V. Wallace, "The DEIMOS Rotation Control System Software," in *Instrument Design and Performance for Optical/Infrared Ground-Based Telescopes*, *Proc. SPIE* **4841**, 2002.
8. D. A. Clarke, S. L. Allen, A. C. Phillips, R. I. Kibrick, V. Wallace, and J. P. Lewis, "Managing DEIMOS removable elements and instrument configuration," in *Instrument Design and Performance for Optical/Infrared Ground-Based Telescopes*, *Proc. SPIE* **4841**, 2002.
9. D. F. Hilyard, G. K. Laopodis, and S. M. Faber, "Chemical reactivity testing of optical fluids and materials in the DEIMOS spectrographic camera for the Keck II telescope," in *Optomechanical Engineering and Vibration Control*, E. A. Derby, C. G. Gordon, D. Vukobratovich, P. R. Yoder, and C. Zweben, eds., *Proc. SPIE* **3786**, pp. 482–492, 1999.
10. C. A. Wright, R. I. Kibrick, and B. Alcott, "CCD imaging systems for DEIMOS," in *Instrument Design and Performance for Optical/Infrared Ground-Based Telescopes*, *Proc. SPIE* **4841**, 2002.
11. S. L. Allen and D. A. Clarke, "Three instruments in four years: the UCO/Lick data-driven toolkit," in *Astronomical Data Analysis Software and Systems. IX*, N. Manset, C. Veillet, and D. Crabtree, eds., *ASP Conference Ser.* **216**, p. 339, 2000.